Biochemistry

Volume 11, Number 16 August 1, 1972

Equilibrium Centrifugation of Nonideal Systems. Molecular Weight Moments for Removing the Effects of Nonideality†

David A. Yphantis* and Dennis E. Roark‡

ABSTRACT: Nonideality, such as that arising from the Donnan effect, perturbs sedimentation–equilibrium concentration distributions so that the measured molecular weights will be erroneously low unless such nonideal effects are properly taken into account. Within certain general limits, the nonideality from the Donnan effect can be expressed as a simple series expansion in integral powers of the concentration, *i.e.*, as a virial expansion of the reciprocals of the number- or weight-average apparent molecular weights. Usually, the effects of the nonideality are limited to one or two virial coefficients, quite often to only the second virial coefficient. Likewise nonideality from excluded volume often appears primarily in the second virial coefficient. Simple derivative transformations of the reciprocal weight or number average molecular weights are shown to generate new averages, the "ideal moments," that are independent of the second nonideal virial coefficient. Other ideal moments are presented that are independent of one or two additional virial coefficients. Thus these moments are not influenced by nonideality whose effects are expressed in the "deleted" virial coefficients. These ideal moments are useful for characterizations of nonideal self-associating systems. In the case of monomer–*n*-mer systems, simple graphical presentations can indicate the monomer molecular weight, the stoichiometry and, for systems in rapid chemical equilibrium, the association constant.

Equilibrium ultracentrifugation, a powerful technique for the study of associating systems of biological macromolecules, is based upon well understood and reasonably simple thermodynamic theory (see, for instance, Goldberg, 1953). In principle, interpretations of sedimentation–equilibrium experiments can be made that are free from the complications encountered with various nonequilibrium techniques (such as gel permeation chromatography or the various hydrodynamic techniques). The fractionation associated with "high-speed" equilibrium ultracentrifugation permits detection and, often, resolution of heterogeneity (Yphantis, 1964; Roark and Yphantis, 1969). Such heterogeneity is often difficult to detect by the other common thermodynamic techniques that exhibit little or no fractionation (*e.g.*, light-scattering, osmotic pressure, or "low-speed, short-column" equilibrium ultracentrifugation).

The power and simplicity of equilibrium ultracentrifugation is sometimes partially negated by the presence of nonideality. By nonideality, here, we mean any (equilibrium) situation leading to a concentration distribution of a macromolecular species that is not of the standard exponential form:

$$c_i(r) = A_i \exp\{\sigma_i r^2/2\} \tag{1a}$$

where, the "reduced molecular weight," σ_i, is

$$\sigma_i = \frac{M_i(1 - \bar{v}_i\rho)\omega^2}{RT} \tag{1b}$$

M_i is the molecular weight of the macromolecular species, $\bar{v}_i$ is its partial specific volume, ρ is the solution density, ω is the angular speed of the rotor, R is the gas constant, and T is the absolute temperature.

† From the Departments of Biophysics and Biology, State University of New York at Buffalo, Buffalo, New York (D. E. R.), and from the Biochemistry and Biophysics Section of the Biological Sciences Group at the University of Connecticut, Storrs, Connecticut (D. A. Y.). *Received March 20, 1972.* This investigation has been supported, in part, by Public Health Service Training Grant 5T1-GM-718-09, and by Research Grants GB-6130, GB-8164, GB-13790, and GB-30825X from the National Science Foundation. A portion of this material was taken from a dissertation submitted by D. E. R. in partial fulfillment of requirements for a Ph.D. degree, State University of New York at Buffalo.

‡ Present address: Department of Biological Chemistry, Milton S. Hershey Medical Center, Hershey, Pa. 17033.

The principle sources of nonideality in equilibrium ultracentrifugation are excluded volume effects and Donnan equilibria. The latter are often encountered in studies of biological macromolecules since these molecules almost always carry a net charge. These macroions cannot sediment independently of their (much lower molecular weight) counterions, thus causing the equilibrium distributions in the centrifugal field to become coupled. Upon sedimentation of these charged macromolecular species, redistribution of the supporting electrolyte must take place in such a way that electroneutrality in every region of the centrifuge cell is maintained and that the supporting electrolyte is itself in thermodynamic equilibrium. The macroion concentration, at sedimentation–equilibrium, is a more slowly increasing function of radial position than it would have been if the macromolecules possessed no net charge. Both the Donnan and excluded volume effects result in the apparent (experimentally observable) molecular weights being less than their true, or ideal, values. Nonideality resulting from the Donnan equilibrium becomes more severe as the charge-to-mass ratio or the concentration of the macromolecular species increases, and as the concentration of the supporting electrolyte decreases.

We have previously developed a thermodynamic description of this Donnan equilibrium for sedimentation–equilibrium of self-associating systems of macromolecules (Roark and Yphantis, 1971). (A self-associating system is one in which identical molecular subunits, monomers, associate to form oligomers.) The applicability of this analysis does not depend on reversibility of the associations, but it does require, however, that the charge-to-mass ratios of all macromolecular species be the same. Thus, if the association does not lead to significant alteration of the charge-to-mass ratio the effects of the coupling of the distributions of macroions and supporting electrolytes can be predicted. Here we present a means of interpreting sedimentation–equilibrium experiments on nonideal systems.

The usual method of interpretation of ultracentrifuge data when nonideality is present involves the extrapolation of the apparent molecular weight averages to zero concentration. While this method has proven useful for determining the molecular weight of a macromolecule in a system that contains only a single macromolecular species, or for determining the monomer molecular weight of a self-associating system, it offers little information about the association process, such as the stoichiometry and equilibrium constants, or about the range of molecular weights present in the centrifuge cell.

Sedimentation equilibrium studies can involve two general approaches. Either the entire concentration distribution can be used in a least-squares-fitting procedure employing the sums of exponentials, modified by terms to account for the nonideality (Haschemeyer and Bowers, 1970; Johnson and Yphantis, 1971); or local regions of the concentration distribution can be successively examined by calculating various local or point-average molecular weights. In the latter approach, the manner in which these point-average moments vary with local concentration or with radial position is then used in an attempt to understand the system. Both approaches are useful and often complement each other. For instance, the point-average method is useful for detection of heterogeneity or associations, and in identifying, under favorable circumstances, the various molecular weight species present. This information can be useful for a least-squares-fitting procedure of the entire concentration distribution to determine the amounts of the various species, or, in the case of a reversibly associating system, the association constants. Here, we continue to employ the point-average method and discuss certain new molecular weight moments useful in the study of nonideal systems.

Alternative techniques using the point-average molecular weights have been suggested in a series of papers by Adams *et al.* (Adams, 1965a,b, 1967; Adams and Filmer, 1966; Adams and Williams, 1964). These techniques involve the simultaneous estimation of the second nonideal virial coefficient and of the parameters associated with the corresponding ideal system (*i.e.*, the various equilibrium constants) from the concentration distribution at sedimentation equilibrium. (The techniques are, in part, based on an integral relation developed by Steiner (1952, 1953a,b) which determines the total monomer weight fraction. Evaluation of these integrals may be difficult if concentration distribution data corresponding to sufficiently low degrees of polymerization are not available.)

Four standard apparent point-average molecular weight moments can usually be evaluated from the concentration distribution at sedimentation equilibrium. These moments have been defined previously (Yphantis, 1964) in terms of apparent reduced molecular weights, or σ's. They are the number-, weight-, Z, and Z + 1 average σ's.

$$\sigma_n(r) \equiv \frac{c(r)}{\int_a^r c(r)d\xi + \frac{c(a)}{\sigma_n(a)}} = \frac{M_{n,a}(r)(1 - \bar{v}\rho)\omega^2}{RT} \tag{2a}$$

$$\sigma_w(r) \equiv \frac{dc(r)/d\xi}{c(r)} = \frac{M_{w,a}(r)(1 - \bar{v}\rho)\omega^2}{RT} \tag{2b}$$

$$\sigma_Z(r) \equiv \frac{d^2c(r)/d\xi^2}{dc(r)/d\xi} = \frac{M_{Z,a}(r)(1 - \bar{v}\rho)\omega^2}{RT} \tag{2c}$$

$$\sigma_{Z+1}(r) \equiv \frac{d^3c(r)/d\xi^3}{d^2c(r)/d\xi^2} = \frac{M_{Z+1,a}(r)(1 - v\rho)\omega^2}{RT} \tag{2d}$$

(where $\xi = r^2/2$ and "a" is some radial distance, usually close to the meniscus. These moments reflect not only the ideal behavior of the system (*i.e.*, the molecular weights of the various species and the associative behavior), but also the nonideal behavior if the system is nonideal. Direct characterization of the system's ideal behavior is not possible with these moments if they are substantially influenced by the nonideality. The new set of local molecular weight averages defined in this paper reflect only the ideal behavior of the system for certain defined and common types of nonideality.

It should be noted that all molecular weight averages mentioned here, including both the standard moments of eq 2 and the ideal moments to be introduced, assume an identical bouyancy factor $(1 - \bar{v}\rho)$ for all solute species. This same assumption was used in our previous derivation of the Donnan effects for self-associating systems. Although this constancy is not an essential assumption, its relaxation would complicate the presentation inordinately: the equivalent Donnan expressions of the form of eq 3 would require a constant ratio of charge to reduced molecular weight, $M_i(1 - \bar{v}_i\rho)$, (or to σ_i) for each species and all expressions involving molecular weight would require rephrasing in terms of the corresponding reduced molecular weight (or σ).

Donnan Equilibria. In this section we present a brief summary of results obtained for the Donnan equilibrium (Roark and Yphantis, 1971). The apparent weight-average molecular

weight, $M_{w,a}$, observed for a charged macroion is given by

$$\frac{1}{M_{w,a}} = \frac{1}{M_{w,I}} + 2B_1c + 3C_1c^2 + 4D_1c^3 + \ldots \quad (3)$$

where B_1, C_1, and D_1 are the nonideal colligative second, third, and fourth virial coefficients, respectively, and where $M_{w,I}$ is the ideal weight-average molecular weight that would have been observed in the absence of any Donnan effect. This modified virial expansion has been shown to be valid unless there is *both* extreme Donnan nonideality and appreciable sedimentation of the supporting electrolyte (in comparison to the sedimentation of the macromolecule).

In most cases, where there is only a moderate amount of nonideality, the only significant contribution arises from B_1, the second nonideal virial coefficient. However, for more extreme cases of nonideality, the higher virial coefficients can become important; which of these higher virial coefficients become important depends upon the stoichiometry of the supporting electrolyte. For example, a monovalent salt of the form BX leads to a positive second and a negative fourth virial coefficient, but to a zero third virial coefficient; while a monodivalent salt leads to a positive second and a positive or negative third virial coefficient but to a zero fourth virial coefficient. The contributions from these higher virial coefficients are invariably much smaller than the contribution from B_1, and, indeed, analysis shows that there is a wide range of concentrations over which the second nonideal virial coefficient is the only practical contributor to the system nonideality.

Equation 3 is not a true virial expansion, since its leading term, $1/M_{w,I}$, is a function of concentration. We could try to express the ideal weight-average molecular weight (or the ideal number-average molecular weight) by a virial expansion whose leading term is the reciprocal monomer molecular weight

$$\frac{1}{M_{w,I}} = \frac{1}{M_1} + 2Bc + 3Cc^2 + 4Dc^3 + \ldots \quad (4)$$

However, this is only partially successful since such expansions for self-associating systems fail to converge except at low degrees of polymerization (Stafford and Yphantis, 1972). In the region of convergence the colligative virial coefficients of eq 4, are related to the various association constants. For example, for a monomer–N-mer system, the first power of concentration to appear in the above expansion is the $N - 1$ power and the virial coefficient for this power will be negative. Thereafter, integral powers of the $N - 1$ power of the concentration occur and the successive nonzero virial coefficients alternate in sign.

Molecular Weight Moments Independent of the Second Virial Coefficient. In this section we consider systems having only moderate nonideality, such that the significant nonideal effects are restricted to contributions from the second virial coefficient. We first examine three molecular weight moments, M_n, M_w, and M_v (defined below) in which the second virial coefficient appears only in the linear term of their series expansions about $c = 0$. (Some molecular weight averages, such as the Z average, contain the second virial coefficient not only in the linear term of their series expansions about $c = 0$, but in all higher terms as well.) Then we define an operation that, when performed on these moments, will generate new moments that are no longer a function of the second virial coefficient.

If C_1 and D_1, the higher nonideal virial coefficients, can be neglected, then we can write an expression for the apparent weight-average molecular weight

$$\frac{1}{M_{w,a}} = \frac{1}{M_{w,I}} + 2B_1c \quad (5)$$

The corresponding virial expansion for the reciprocal number-average molecular weight may be generated from eq 4 or 5 by using a relationship between $M_n(c)$ and $M_w(c)$

$$\frac{1}{M_w(c)} = \frac{d\left(\frac{c}{M_n(c)}\right)}{dc} \quad (6)$$

This relation may be derived by expressing the two molecular weight averages in terms of ratios of radial derivatives of the concentration (Yphantis, 1964; see also Adams, 1965a). Thus, from eq 5 and 6, $1/M_{n,a}$ must be given by

$$\frac{1}{M_{n,a}} = \frac{1}{M_{n,I}} + B_1c \quad (7)$$

We define a new moment that is related to $1/M_w$ in the same way that eq 6 relates $1/M_w$ to $1/M_n$

$$\frac{1}{M_v} \equiv \frac{d\left(\frac{c}{M_w}\right)}{dc} \quad (8)$$

From eq 7 and 8, we infer that

$$\frac{1}{M_{v,a}} = \frac{1}{M_{v,I}} + 4B_1c \quad (9)$$

The reciprocals of each of these three moments, M_n, M_w, and M_v, are separable into an ideal term and an additive nonideal virial expansion in which the second nonideal colligative virial coefficient, B_1, occurs only in the term that is linear in concentration. The following differential operation, when performed on any one of these moments, generates a new moment independent of B_1. These new moments, the so called ideal moments, are defined by

$$\frac{1}{M_{y1}} \equiv \frac{d\left(\frac{1}{cM_n}\right)}{d\left(\frac{1}{c}\right)} \quad (10a)$$

$$\frac{1}{M_{y2}} \equiv \frac{d\left(\frac{1}{cM_w}\right)}{d\left(\frac{1}{c}\right)} \quad (10b)$$

$$\frac{1}{M_{y3}} \equiv \frac{d\left(\frac{1}{cM_v}\right)}{d\left(\frac{1}{c}\right)} \quad (10c)$$

For a nonideal system with $B_1 \neq 0$, these new ideal moments will assume the same values that they would have exhibited

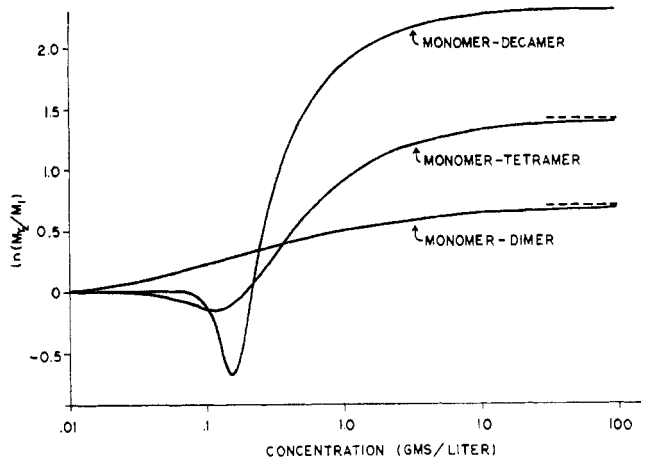

FIGURE 1: Variation of the ideal moment M_{y2} with concentration. The behavior of this moment is shown for monomer–dimer, monomer–tetramer, and monomer–decamer associations. M_{y2} is presented in terms of ln M_{y2} *vs.* ln c, so that the shapes of the resulting curves do not depend on either the molecular weight of the monomer, M_1, or on the association constant (see text). (The association constants K_a are 10 l./g, 50 l.^{3}/g^3 and 2×10^6 l.^{9}/g^9 for the monomer–dimer, monomer–tetramer, and monomer–decamer systems, respectively.)

for the corresponding (hypothetical) ideal system, where $B_1 = 0$.

In the Appendix, we show that M_{y1}, M_{y2}, and M_{y3} are related in the same fashion as are M_n, M_w, and M_v, namely

$$\frac{1}{M_{y2}} = \frac{d\left(\frac{c}{M_{y1}}\right)}{dc} \tag{11a}$$

$$\frac{1}{M_{y3}} = \frac{d\left(\frac{c}{M_{y2}}\right)}{dc} \tag{11b}$$

The Appendix also derives relations between the ideal moments and the standard moments (M_n, M_w, M_Z, and M_{Z+1})

$$\frac{1}{M_{y1}} = \frac{2}{M_n} - \frac{1}{M_w} \tag{12a}$$

$$\frac{1}{M_{y2}} = \frac{M_Z}{M_w^2} \tag{12b}$$

$$\frac{1}{M_{y3}} = \frac{M_Z}{M_w^3}\left[M_{Z+1} - 3M_Z + 3M_w\right] \tag{12c}$$

Relation 12a is particularly instructive: comparison of this to the virial expansions of eq 5 and 7 makes apparent that these two virial expansions have been linearly combined to eliminate the second virial coefficient.

As an indication of the behavior of these moments, Figure 1 presents values of M_{y2} *vs.* concentration on a log–log scale, for different degrees of polymerization. One unusual aspect of these moments is that, for monomer–trimer and higher degrees of polymerization, these ideal moments exhibit a decrease below the monomer molecular weight. Similar decreases are exhibited by all ideal moments presented here. The minimum values of the moments resulting from this decrease occur at low values of α (the weight fraction of solute that is associated): at values of α less than 0.15 for M_{y1} and less than 0.07 for M_{y2}. The higher the degree of polymerization, the greater will be this decrease. For example, the minima of the monomer–trimer curves drop to 97% and 95% of monomer molecular weight for M_{y1} and M_{y2}, respectively; while that of a monomer–decamer curve decrease to 77 and 51% of M_1 for M_{y1} and M_{y2}, respectively. The origin of this decrease can be appreciated by examining the virial expansions of these ideal moments. These expansions, valid at low α, can be generated from eq 4 and 10, and the corresponding equations for M_n and M_v (see eq 16). One notes that the third and higher virial coefficients in the expansions of the three ideal moments occur in the expansions with negative signs, contrary to the way in which they occur in the expansions of the standard moments. Now, for a monomer–N-mer system, the first (ideal) virial coefficient that is non-zero other than the $1/M_1$ term, is the N-th, which will be negative. It is this virial coefficient term that is the dominating term at low values of α; and it is this term that causes a decrease in the moment below the monomer value. Whether these decreases will prove helpful in identifying stoichiometries is as yet uncertain. Caution should be used in the interpretation of experimental data, lest these decreases lead one to falsely conclude that the molecular weight of a species is lower than the actual M_1. Simple estimation of monomer molecular weight from direct observation of M_{y2}, for example, will yield *underestimates* if a sufficiently low weight fraction of monomer is not observable. Other methods should then be used to obtain estimates of M_1. One of the most useful of these methods makes use of the characteristic shapes obtained in such log–log plots as Figure 1 and will be discussed in a later section. The most significant (*i.e.*, the deepest) decreases in these moments are also the ones most sharply confined to a moderate range in concentration. If we consider the point at which $M_{y2}(\alpha)$ ranges from values less than M_1 to greater than M_1, we find that this occurs only for α less than 0.2 for all monomer–N-mer systems. In particular for values of N between 3 and 23, this crossover point is between $\alpha = 0.15$ and 0.2. However, for the higher degrees of polymerization, α increases much more rapidly with concentration, thus causing the decrease below M_1 to be confined to a smaller concentration range.

It should be noted that the values of M_{y2} for a monomer–dimer system, when presented as a function of concentration, approach the ordinate with a zero slope, contrary to the behavior of the standard moments that have limiting slopes that are positive and finite. This zero slope arises from the complete absence of any linear term in the virial expansions of these ideal moments. Figure 2 compares M_{y1}, M_{y2}, and M_{y3} for a monomer–tetramer system. At a given concentration $M_{y3} > M_{y2} > M_{y1}$, except in the region of the decreases below M_1. Note that this decrease occurs at lower values of α (or, of concentration) and is more pronounced for M_{y3} than for M_{y2}, and for M_{y2} than for M_{y1}. For reference, $M_{w,I}$ has also been included. Both M_{y1} and M_{y2} are always less than $M_{w,I}$, and thus reflect more strongly the presence of low molecular weight species. The values of M_{y1} also are always less than the ideal number-average molecular weight.

An interesting property of M_{y3} is evident in Figure 2: a rise above the molecular weight of the N-mer. This rise does not occur for a monomer–dimer or a monomer–trimer system. At higher values of N (the degree of polymerization), the behavior of M_{y3} becomes increasingly more complicated.

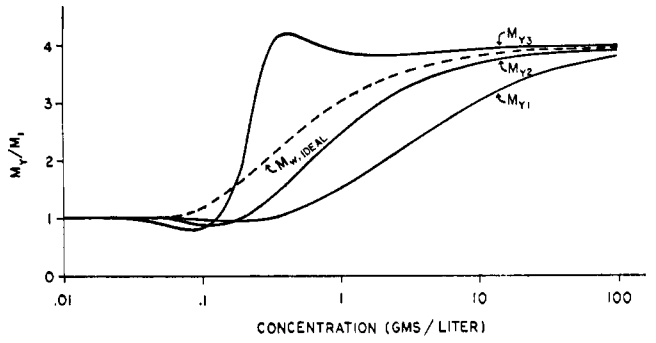

FIGURE 2: Behavior of ideal moments for a monomer–tetramer system. The ideal moments M_{y1}, M_{y2}, and M_{y3}, are presented as a function of ln c for a nonideal monomer–tetramer system in which the nonideality is restricted to the second virial coefficient. The shapes of the curves are independent of the particular association constant. For reference, values of $M_{w,I}$ are also presented for the corresponding ideal system. (K_n = 50 l.^{3}/g^3).

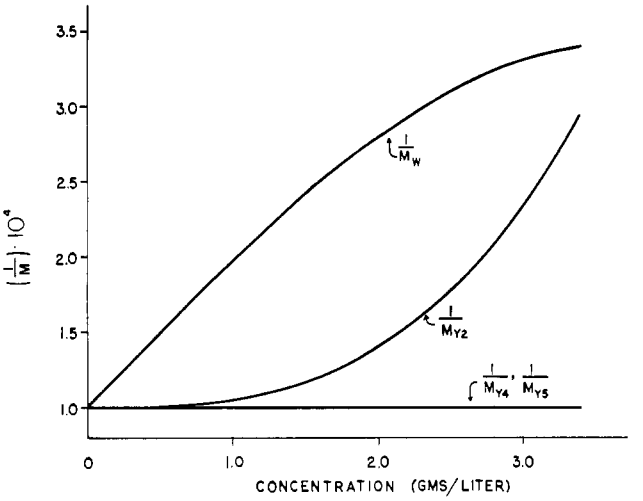

FIGURE 3: A monodisperse system with nonideality in both the second and the fourth virial coefficients. Values of M_w, M_{y2}, M_{y4}, and M_{y5} are presented for a system in which the nonideal second-virial coefficient B_1 = 5 × 10^{-5} l. mole/g^2, and the nonideal fourth-virial coefficient D_1 = −6.25 × 10^{-7} l.^{3} mole/g^4. This corresponds to the Donnan nonideality for a macromolecular species having a molecular weight of 10,000 and an average effective charge of 4.5, in the presence of a uni-univalent supporting electrolyte having a concentration of $m_{3,0}$ = 0.001 m. Values of $M_{w,app}$ are affected by both B_1 and D_1; values of M_{y2} only by D_1; while M_{y4} and M_{y5} are uninfluenced by the nonideality.

For systems having a degree of polymerization of six or greater, two singularities occur in M_{y3}. For these higher degrees of polymerization, M_{y3} can be thought to be an ill-behaved function. Its peculiarities are difficult to relate intuitively to the properties of the system under investigation. The chief virtue of M_{y3} is its use as an intermediate quantity in the calculation of other ideal moments that will be discussed in the next section. These singularities do not afford a problem in the calculation or in the use of M_{y3} in deriving these other moments, since what is calculated and used is not M_{y3} itself, but its reciprocal, which possesses no singularities but only zeros.

Other Ideal Moments. Although there is a wide range of macroion concentrations for which only the second nonideal virial coefficient need be considered, conditions of extreme nonideality sometimes make it necessary to take into account the third or the fourth virial coefficient. (One will remember that for a uni-univalent electrolyte the third nonideal virial coefficient will be zero and the fourth negative; while for a mono-divalent salt, the third will be non-zero, and the fourth zero.) For a monovalent salt, the second nonideal virial coefficient always causes a decrease in the values of the standard moments (M_n, M_w, M_Z, and M_{Z+1}), while for a uni-univalent salt the effect (at higher solute concentrations) of the fourth nonideal virial coefficient will be to lessen the extent of this decrease. Thus, if $1/M_{w,a}$ for a monodisperse system is examined as a function of concentration (see Figure 3), the initial positive slope arises from the nonideal second virial coefficient. However, the curvature that reduces this slope at the higher concentrations reflects the presence of a nonideal fourth virial coefficient. The direction of the change in slope of this function is such that it might easily be mistaken for the presence of larger molecular weight species. The nonideal fourth virial coefficient causes the reciprocal of the ideal moments (M_{y1} and M_{y2}) to increase at higher concentrations (see Figure 3). This is in contrast to the effect of this coefficient on the behavior of the standard moments, and results from the fourth virial coefficient that appears in the virial expansions of the ideal moments with a negative sign.

We have treated the case in which the nonideality was confined to the second virial coefficient by defining molecular weight moments that were independent of the second virial coefficient. Similarly, we can define moments independent of both the second and the fourth nonideal virial coefficients that will be useful in examining highly nonideal systems whose supporting electrolyte is a uni-univalent salt. This readily can be done using linear combinations of the three reciprocal ideal moments previously defined. These linear combinations are chosen so that they have $1/M_1$ as their leading term, and so that they contain no cubic term in concentration. Two such linear combinations define M_{y4} and M_{y5}.

$$\frac{1}{M_{y4}} \equiv \frac{4}{3}\frac{1}{M_{y1}} - \frac{1}{3}\frac{1}{M_{y2}} \tag{13a}$$

$$\frac{1}{M_{y5}} \equiv \frac{4}{3}\frac{1}{M_{y2}} - \frac{1}{3}\frac{1}{M_{y3}} \tag{13b}$$

Figure 3 shows the values of $1/M_{y4}$ and $1/M_{y5}$ for this nonideal monodisperse system. The behavior of M_{y1}, M_{y2}, M_{y4}, and M_{y5} for a monomer–trimer system with pronounced nonideality in both the second and the fourth virial coefficients is shown in Figure 4. The values of M_{y4} and M_{y5} are unaffected by the nonideality; on the other hand, M_{y1} and M_{y2} are decreased by the negative nonideal fourth virial coefficient. There is usually little advantage in using M_{y4} and M_{y5} when the nonideality is reasonably confined to the second virial coefficient since the calculation of M_{y4} and M_{y5} is generally less precise than the calculation of either M_{y1} or M_{y2}. In any case, Figure 4 also presents in dashed lines the ideal values of M_{y1} and M_{y2} for comparison. These ideal values of M_{y1} and M_{y2} correspond to the values expected when all nonideality is manifest strictly in the second virial coefficient. Note that, except in the region of the decrease below M_1, the values of M_{y4} are lower than the values of the other three moments shown; and that the values of M_{y5} are lower than the values of M_{y2}.

We need not be concerned with any nonideal fourth virial coefficient in a system where the supporting electrolyte is a

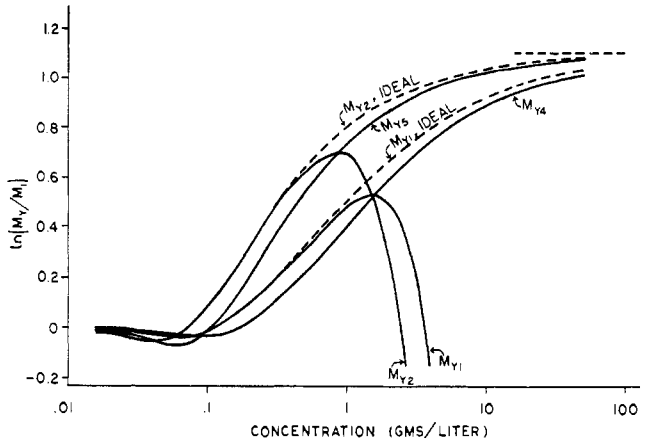

FIGURE 4: An associating system with nonideality in the second and fourth virial coefficients. Values of the ideal moments M_{y1}, M_{y2}, M_{y4}, and M_{y5} are presented for a nonideal monomer–trimer system. This is the same system presented in Figure 3, except that here the monomer associates to form trimers. Values of M_{y1} and M_{y2} are influenced by the fourth-virial nonideality but values of M_{y4} and M_{y5} are not affected. For reference, values of $M_{y1,I}$ and $M_{y2,I}$ are presented for the corresponding system in which $D_1 = 0$. ($K_a = 50\ l.^2/g^2$).

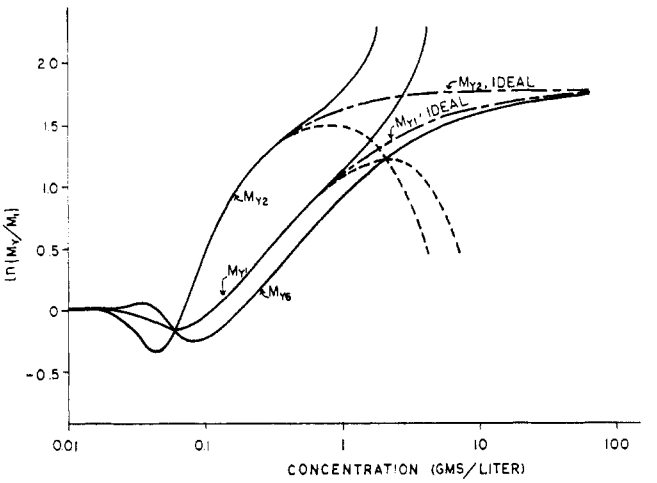

FIGURE 6: An associating system with nonideality in the second and third virial coefficients. Same system as presented in Figure 5, except that here the monomer is involved in a monomer–hexamer association. The values of M_{y1} and M_{y2} are influenced by the nonideality from the third virial coefficient. The direction of the deviation from their ideal values (also presented) depends on the sign of the product of the charge on the macromolecule and on the divalent ion. The solid lines and dashed lines refer to a positive and negative product, respectively. Values of M_{y6} are not affected by the nonideality ($K_a = 5 \times 10^5\ l.^5/g^5$).

mono-divalent salt. However, for sufficiently large macromolecular concentration, the nonideal third virial coefficient may become important (see Roark and Yphantis, 1971). Analogous to the above, we now define two moments, M_{y6} and M_{y7}, through linear combinations of the reciprocals of M_{y1}, M_{y2}, and M_{y3} so that these new moments become independent

$$\frac{1}{M_{y6}} = \frac{3}{2}\frac{1}{M_{y1}} - \frac{1}{2}\frac{1}{M_{y2}} \tag{14a}$$

$$\frac{1}{M_{y7}} \equiv \frac{3}{2}\frac{1}{M_{y2}} - \frac{1}{2}\frac{1}{M_{y3}} \tag{14b}$$

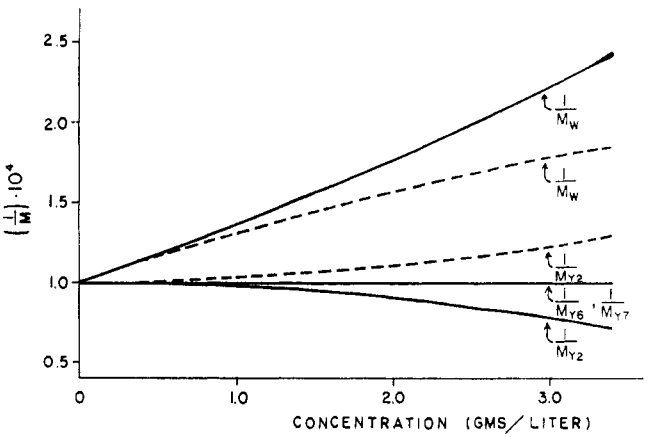

FIGURE 5: A monodisperse system with nonideality in the second and third virial coefficients. Behavior of the same system as presented in Figure 3, except that here the supporting electrolyte is a mono-divalent salt. Values of $M_{w,app}$ are affected by both B_1 and C_1; values of M_{y2}, only by C_1. In contrast, values of M_{y6} and M_{y7} are uninfluenced by the nonideality. The directions of the deviations in M_w and M_{y2}, due to the third-virial nonideality, depend on the sign of the product of the charge on the macromolecule and the charge on the divalent ion. The solid lines for these two moments refer to the product having a negative sign, and the dashed lines to a positive sign.

of the second and third virial coefficients. Figure 5 shows the behavior of various moments for a highly nonideal, monodisperse system in a solvent whose supporting electrolyte is a mono-divalent salt. There are nonideal contributions to both the second and third virial coefficients. Note that the direction of the deviations from ideal values depends on the sign of the product of the charge on the macromolecule and the charge on the divalent ion. The constant value of M_{y6} and M_{y7} (equal to the molecular weitht of the monomer) is also shown for this nonideal monodisperse system. The behavior of a highly nonideal associating system in the presence of a mono-divalent salt is illustrated in Figure 6. This monomer–hexamer system has nonideal second and third virial coefficients. The values of M_{y6} are unaffected by this nonideality; however, M_{y1} and M_{y2}, from which M_{y6} is derived, are perturbed at higher concentrations by the nonideal third virial coefficient. The direction of the deviations from their ideal values depends on the sign of the product of the charge on the macromolecule and the charge on the divalent ion. All four moments (M_{y4}, M_{y5}, M_{y6}, and M_{y7}) display decreases below the monomer value, for N equal to three or greater, at low values of α. In addition, M_{y4} and M_{y5} exhibit a small initial rise above monomeric molecular weight for monomer–N-mer systems where N is 5 or more; M_{y6} and M_{y7} will have the increases for N equal to 4 or more. The extent of the initial increase above the molecular weight value of the monomer, as well as the extent of the subsequent decrease below this monomeric molecular weight, is greater for M_{y7} than it is for M_{y6}. Except in the region of the irregularities at low values of α, the values of M_{y7} are always greater than the values of M_{y1} or M_{y6}, but less than the values of M_{y2}.

We have seen that by using any two of the basic ideal moments we can remove an additional virial coefficient. Similarly, if all three moments are used, one further virial coefficient may be eliminated. Such a procedure may be useful for situations more complex than considered so far, situations where it is desirable to eliminate nonideal contributions to

the second, third, and fourth virial coefficients, for instance. A moment, M_{y8}, independent of these virial coefficients may be generated from M_{y1}, M_{y2}, and M_{y3}. This moment is illus-

$$\frac{1}{M_{y8}} \equiv \frac{2}{M_{y1}} - \frac{7}{6}\frac{1}{M_{y2}} + \frac{1}{6}\frac{1}{M_{y3}} \tag{15}$$

trated in Figure 7 for a monomer–tetramer system.

For low values of α, where series expansions of the standard moments are valid, we may express the ideal moments in terms of series expansions corresponding to eq 4. Thus

$$\frac{1}{M_{y1}} = \frac{1}{M_1} - Cc^2 - 2Dc^3 - 3Ec^4 + \ldots \tag{16c}$$

$$\frac{1}{M_{y2}} = \frac{1}{M_1} - 3Cc^2 - 8Dc^3 - 15Ec^4 + \ldots \tag{16b}$$

$$\frac{1}{M_{y3}} = \frac{1}{M_1} - 9Cc^2 - 32Dc^3 - 75Ec^4 + \ldots \tag{16c}$$

$$\frac{1}{M_{y4}} = \frac{1}{M_1} - \frac{1}{3}Cc^2 + Ec^4 + \ldots \tag{16d}$$

$$\frac{1}{M_{y5}} = \frac{1}{M_1} - Cc^2 + 5Ec^4 + \ldots \tag{16e}$$

$$\frac{1}{M_{y6}} = \frac{1}{M_1} + Dc^3 + 3Ec^4 + \ldots \tag{16f}$$

$$\frac{1}{M_{y7}} = \frac{1}{M_1} + 4Dc^3 + 15Ec^4 + \ldots \tag{16g}$$

$$\frac{1}{M_{y8}} = \frac{1}{M_1} - Ec^4 + \ldots \tag{16h}$$

Evaluations of the ideal moments discussed so far require knowledge of the concentration at each point; the values of the concentration gradient alone are insufficient for their calculation. It is useful to have an ideal moment that requires knowledge only of the concentration gradient. If we define M_{y0} as

$$M_{y0} \equiv M_{y2}[{}^3/_2 - {}^1/_2 M_{y2}/M_{y3}]^2 \tag{17}$$

it is clear that M_{y0} is a moment independent of the nonideal second virial coefficient, B_1. Combining eq 16 and 21, one can show that M_{y0} is also given by

$$M_{y0} = M_Z[{}^3/_2 - {}^1/_2 M_{Z+1}/M_Z]^2 \tag{18}$$

Equation 18 shows this moment to be a function of only M_Z and M_{Z+1}; and evaluation of these two standard moments requires only a knowledge of the concentration gradient at a series of radii. Estimates of M_{y0} are thus independent of any additive constant and depend only on the gradient. Figure 7 presents values of this moment for a monomer–tetramer system. It should be noted that this moment shows decreases below the molecular weight of the monomer for all monomer–N-mer systems with N equal to or greater than three.

The decrease below monomer molecular weight is more broad for M_{y8} than for any other ideal moment. For the monomer–tetramer case (see Figure 7), M_{y8} does not finally cross over the monomer molecular weight value until the system is 60% associated. On the other hand, M_{y0} crosses over the monomer molecular weight at only 9% associated. For comparison, the crossover points for this monomer–tetramer system for M_{y1} and M_{y2} are 34 and 18% associated, respectively. As a further indication of differences in behavior of M_{y8} and M_{y0}, note that at the crossover point for M_{y8}, where it assumes a value equal to the monomer molecular weight, the value of M_{y0} is 82% of the tetramer molecular weight. In general, for systems with nonideal second virial coefficients, the family of moments shown in Figure 7 is analogous to the family of standard moments (M_n, M_w, M_Z, and M_{Z+1}) for an ideal system insofar as the various moments have different sensitivities to the relative amounts of high or low molecular weight species present in a mixture.

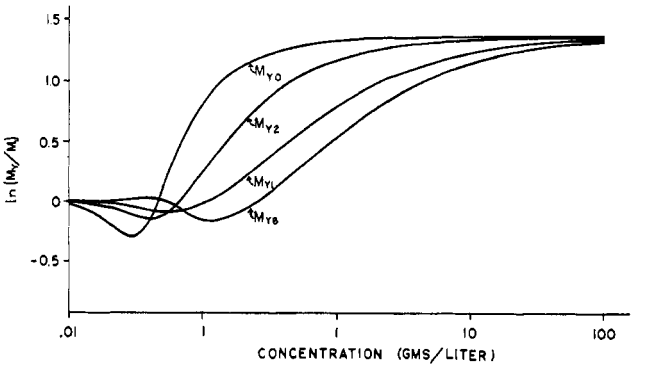

FIGURE 7: Variation of four ideal moments for a monomer–tetramer system. The moments, M_{y8}, M_{y1}, and M_{y0}, are presented in the form ln M_y *vs.* ln c for a nonideal monomer–tetramer system in which the nonideality is restricted to the second virial coefficient. The shapes of the curves are independent of either the monomer–molecular weight, M_1, or of the association constant ($K_a = 10^3$ l.^{3}/g^3).

Calculation Procedures. Detailed calculation procedures used to calculate both the standard moments and these ideal moments, along with related procedures for determining the zero-concentration level, for smoothing experimental data, and for choosing the integration constant needed to calculate the number-average molecular weight will be presented in a future paper. Here, we present an outline of the procedure and of the various functional forms that have proven most advantageous for calculation of these ideal moments. First we calculate the weight-average σ's.

$$\sigma_w(r) = \frac{\mathrm{d} \ln c(r)}{\mathrm{d}(r^2/2)} \tag{19}$$

After the complete set of σ_w's has been determined, σ_{y2} is calculated at each point

$$\frac{1}{\sigma_{y2}(c)} = \frac{\mathrm{d}\left(\frac{1}{c\sigma_w(c)}\right)}{\mathrm{d}\left(\frac{1}{c}\right)} \tag{20}$$

The values of σ_w are also used to calculate the number-average σ at each radius

$$\sigma_n(r) = \frac{c(r)}{\int_{c(a)}^{c(r)} \frac{\mathrm{d}c}{\sigma_w(c)} + \frac{c(a)}{\sigma_n(a)}} \tag{21}$$

where the radius a occurs near 100 μ of fringe displacement. Values of σ_n and σ_w are combined to calculate σ_{y1}

$$\frac{1}{\sigma_{y1}(r)} = \frac{2}{\sigma_n(r)} - \frac{1}{\sigma_w(r)} \tag{22}$$

The last of the basic ideal moments is found using the previously calculated values of σ_{y2}

$$\frac{1}{\sigma_{y3}(c)} = \frac{1}{\sigma_{y2}(c)} + \frac{d\left(\frac{1}{\sigma_{y2}(c)}\right)}{d \ln c} \tag{23}$$

This relation can be derived from eq 11b.

Linear combinations of values of σ_{y1}, σ_{y2}, and σ_{y3}, according to eq 13–15, then yield values for moments independent of any higher virial coefficients. Finally, estimates of σ_{y0} are obtained from the analog of eq 17

$$\sigma_{y0} = \sigma_{y2}[^3/_2 - {}^1/_2\sigma_{y2}/\sigma_{y3}]^2 \tag{24}$$

(It should be noted that even if the values of σ_{y2} and σ_{y3}, used in eq 24, are systematically in error due to a constant additive error in the concentrations, this error is not propagated to σ_{y0}.)

It is interesting to note the similarity between the calculation of σ_{y2} and σ_Z. Equation 20 may be written as

$$\frac{1}{\sigma_{y2}} = \frac{d\left(\frac{1}{dc/d\xi}\right)}{d(1/c)} \tag{25}$$

where $\xi = r^2/2$. Thus a graph of the reciprocal of the gradient $dc/d\xi$ *vs.* the reciprocal of the concentration has a local slope equal to the inverse of σ_{y2}. Compare this to the standard procedure (Van Holde and Baldwin, 1958), for obtaining estimates of σ_Z as the slope of a graph of $dc/d\xi$ *vs.* the concentration.

Detection of Heterogeneity. Previously, we have discussed in detail heterogeneity and its detection by sedimentation equilibrium (Yphantis, 1964; Roark and Yphantis, 1969). We consider a system to be heterogeneous here if the macromolecular solute consists of more than one thermodynamic component. Thus a heterogeneous solute might consist of an associating system contaminated by the presence of unrelated macromolecular species or by the presence of other forms of the same solute that are not in thermodynamic equilibrium, such as irreversibly aggregated solute molecules or forms of the solute that exhibit different association constants (Johnson and Yphantis, 1971). Associating systems that chemically reequilibrate slowly compared to the time period of the experiment will exhibit apparent heterogeneity. Observational techniques that produce no fractionation of the thermodynamic components yield measured molecular weights that are still a function only of total concentration, making detection of such heterogeneity difficult and dependent on a specific model for the system. However, as first noted by Squire and Li (1961), equilibrium ultracentrifugation should lead to fractionation of the thermodynamic components of a heterogeneous system (*i.e.*, the solute composition, in terms of thermodynamic components, becomes a function of the radius). The extent of such fractionation is greater the higher the speed or the longer the column height. If the speed is made sufficiently great, however, the large gradients in the most centrifugal region of the cell preclude observations there, thus perhaps obscuring detection of higher molecular weight components. On the other hand, an increased column height will increase the time required to reach equilibrium. In any case, in the absence of pressure effects, column heights longer than those necessary to essentially deplete the meniscus region of macromolecular species afford little additional information about the heterogeneity of the system.

In the case of heterogeneous systems studied by equilibrium ultracentrifugation at high speeds (apparent σ's on the order of 2–6), and sufficiently long columns (we normally employ a column height of 3 mm), the observed molecular weights should depend on position as well as on total solute concentration (Squire and Li, 1961; Yphantis, 1964; Roark and Yphantis, 1969). Thus, experiments at different initial loading concentrations can be used to test for heterogeneity: graphs of any point-average molecular weight, $M(r)$, as a function of the equilibrium solute concentration at the point r, $c(r)$, should give a single curve for all loading concentrations if the solute is a single thermodynamic component.[1] However, if the system is sufficiently heterogeneous, the curves will diverge. We wish to emphasize that in the above plot $M(r)$ may be any of the standard or ideal moments, regardless of whether the system is nonideal.

Graphical Method for Examining Nonideal Monomer–N-mer Systems. There exists a simple method, which uses the standard molecular weight moments to determine the stoichiometry and monomer molecular weight of an ideal monomer–N-mer system (this method has been independently discovered a number of times: Sophianopoulos and Van Holde, 1964; Teller *et al.*, 1969; Roark and Yphantis, 1969). This "two-species plot" technique can be extended to nonideal systems if the nonideality is not too severe (see Roark and Yphantis, 1969). There appears to be no simple equivalent technique using the ideal moments for the study of nonideal systems. Here we present a somewhat more laborious technique which utilizes the concentration dependence of the ideal moments. We wish to find some plot whose shape depends only on the stoichiometry, and hence will be indicative of that stoichiometry, and not of the equilibrium constant. If the weight fraction polymerized, α, or any quantity that is a function of α alone, and not of the equilibrium constant or amount of a species, is presented as a function of ln c, the shape of such a graph will depend only on the stoichiometry. To show this, consider the equilibrium constant, on a weight-concentration basis, for a monomer–N-mer system

$$K = \frac{\alpha c}{[(1 - \alpha)c]^N} \tag{26}$$

This can be rearranged to give

$$\ln\left[\frac{\alpha}{(1 - \alpha)^N}\right] = (N - 1) \ln c + \ln K \tag{27}$$

From the last equation, it is evident that if α is presented *vs.* ln c, for a given degree of polymerization, the shapes will be the same for all values of the equilibrium constant. The var-

[1] Note that one must exclude possible perturbations from pressure dependence, or from potential differences in solute composition arising either from redistribution of solvent components or from inappropriate sample preparation.

ious graphs for different values of K can be made to superimpose by merely transposing them along the ln c axis.

For a given stoichiometry, M_y/M_1 is a function only of α and the degree of polymerization, N. Thus, graphical presentations of M_y/M_1 *vs.* ln c for any of the ideal moments can be superimposed with reference or calculated curves for the same stoichiometries by translation along the ln c axis. Stoichiometries can be identified by comparison of such experimental graphs to a catalog of graphs calculated for various stoichiometries.

The translation along the ln c axis will be a measure of the equilibrium constant if the system is in a thermodynamic equilibrium governed by eq 26, or a measure of the relative amounts of the two species present through an "apparent equilibrium constant" if the two species are not in a chemical equilibrium. If the catalogued curve represents a system with an equilibrium constant of K_0, and if a translation Δ ln c has been performed, then consideration of eq 27 shows that the association constant of the experimental system is given by

$$\ln K = \ln K_0 - (N - 1)\Delta \ln c \tag{28}$$

The above method requires knowledge of the monomer molecular weight. An alternative is to graph ln M_y *vs.* ln c. Here, too, the shapes of such curves will depend only on the degree of polymerization. In addition to translation along the ln c axis to account for different equilibrium constants, a translation along the ln M_y axis is also necessary to account for different monomer molecular weights. (Rotation is not a permissible operation.) The extent of translation Δ ln M along the ln M_y axis is a measure of the monomer molecular weight. If the molecular weight of the monomer used to calculate the catalog curve is M_1^0, then the monomer molecular weight of the experimental system will be given by

$$\ln M_1 = \ln M_1^0 + \Delta \ln M \tag{29}$$

Other methods may better estimate the equilibrium constants once the stoichiometry and monomer molecular weight are known. For example, one alternative is to use one of the ideal moments to determine the values of $\alpha(c)$ for the set of concentrations corresponding to the experimental points. (This can be done graphically by using a presentation of calculated values of M_y/M_1 *vs.* α for the appropriate stoichiometry.) Once α has been determined as a function of concentration, the equilibrium constant may be found by a graph of $\alpha/(1 - \alpha)^N$ *vs.* c^{N-1}. The equilibrium constant will be the slope of such a plot (see Roark and Yphantis, 1969).

Definite stoichiometric analysis of nonideal systems containing more than two macromolecular species is at present not generally feasible. However, it is often possible to detect the existence of more than two species, even if the several molecular weights and equilibrium constants are not readily determinable. In principle it should be possible to analyze nonideal self-associating systems consisting of more than two species, if enough experiments are performed under various experimental conditions where different species are in abundance. Naturally, if the presence of several molecular species does not arise from reversible chemical equilibria of a single thermodynamic solute, but rather from heterogeneity, additional purification should precede further characterization by equilibrium ultracentrifugation.

Appendix

Derivations of Some Relations between the Moments. The ideal moments, M_{y1}, M_{y2}, and M_{y3} are defined by eq 10. Here, we first derive the relations of eq 12, relating the ideal moments to the standard molecular weight moments. From the definition of M_{y1} (eq 10a) we can obtain

$$\frac{1}{M_{y1}(c)} = \frac{1}{M_n(c)} - \frac{d[1/M_n(c)]}{d \ln c} \tag{A1}$$

On the other hand, from eq 6, we can infer that

$$\frac{d[1/M_n(c)]}{d \ln c} = \frac{1}{M_w(c)} - \frac{1}{M_n(c)} \tag{A2}$$

The combination of eq A1 and A2 yields eq 12a.

Equation 12b may be demonstrated by using an expression for M_Z (see Van Holde and Baldwin (1958) and the definition of $\sigma_{w,app}$):

$$M_Z(c) = \frac{d[cM_w(c)]}{dc} \tag{A3}$$

Also, from the definition of M_{y2} (eq 10b)

$$\frac{1}{M_{y2}(c)} = \frac{1}{M_w^2(c)} \frac{d[cM_w(c)]}{dc} \tag{A4}$$

and combination of eq A3 and A4 yields eq 12b.

Finally, to derive the last of eq 12, we first find an expression for M_v in terms of the standard moments. From eq 8, we can obtain the relation

$$\frac{1}{M_v(c)} = \frac{1}{M_w(c)} - \frac{1}{M_w^2(c)} \frac{dM_w(c)}{d \ln c} \tag{A5}$$

Equation A3 may be rewritten as

$$M_Z(c) = M_w(c) + \frac{dM_w(c)}{d \ln c} \tag{A6}$$

and the combination of eq A5 and A6 gives

$$\frac{1}{M_v} = \frac{2}{M_w} - \frac{M_Z}{M_w^2} \tag{A7}$$

It is interesting to note that eq A7 can be written in a manner that is analogous to eq 12a

$$\frac{1}{M_{y2}} = \frac{2}{M_w} - \frac{1}{M_v} \tag{A8}$$

Substituting eq A7 into the defining relation for M_{y3}, eq 12c; and using eq A3, we find, after some simplification that

$$\frac{1}{M_{y3}} = \frac{M_Z}{M_w^2}\left[3 - 2\frac{M_Z}{M_w}\right] + \frac{1}{M_w^2} \frac{d M_Z}{d \ln c} \tag{A9}$$

To proceed further, we require an expression involving the derivative of M_z analogous to eq A3. Such a relation may be

easily derived by expressing the standard moments as ratios of radial derivatives of the concentration. Then

$$M_{z+1} = \frac{d(cM_wM_z)}{d(cM_w)} \quad (A10)$$

Combination of eq A9 and A10 then yields the desired eq 12c.

Next, we wish to obtain the derivative relations of eq 11 that relate the concentration dependence of one ideal moment to the next higher moment. From eq 12a we find that

$$\frac{d[c/M_{y1}(c)]}{dc} = \frac{2d[c/M_n(c)]}{dc} - \frac{d[c/M_w(c)]}{dc} = \frac{2}{M_w} - \frac{1}{M_v} \quad (A11)$$

where the equality on the right results from eq 10 and 12. A comparison of this result to eq A8 immediately verifies eq 11.

Finally, in order to demonstrate eq 11b, we start with eq 12b, and obtain the result

$$\frac{d[c/M_{y2}]}{dc} = \frac{M_z}{M_w^2} + \frac{1}{M_w^2 d\ln c}\frac{dM_z}{} - 2\frac{M_z}{M_w^3 d\ln c}\frac{dM_w}{} \quad (A12)$$

Substitution of eq A6 and A10 then gives us

$$\frac{d[c/M_{y2}]}{dc} = \frac{M_z}{M_w^3}(M_{z+1} - 3M_Z + 3M_w) \quad (A13)$$

and a comparison of eq A13 and 12c leads to the desired relation, eq 11b.

References

Adams, E. T., Jr. (1965a), *Biochemistry 4*, 1655.
Adams, E. T., Jr. (1965b), *Biochemistry 4*, 1646.
Adams, E. T., Jr. (1967), *Biochemistry 6*, 1864.
Adams, E. T., Jr., and Filmer, D. L. (1966), *Biochemistry 5*, 2971.
Adams, E. T., Jr., and Williams, J. W. (1964), *J. Amer. Chem. Soc. 86*, 3454.
Goldberg, R. J. (1953), *J. Phys. Chem. 57*, 194.
Haschemeyer, R. H., and Bowers, W. F. (1970), *Biochemistry 9*, 435.
Johnson, M. L., and Yphantis, D. A. (1971), *Abstr. 15th Annu. Meeting Biophys. Soc.*, WPM-H18.
Roark, D. E., and Yphantis, D. A. (1969), *Ann. N. Y. Acad. Sci. 164*, 245.
Roark, D. E., and Yphantis, D. A. (1971), *Biochemistry 10*, 3241.
Sophianopoulos, A. J., and Van Holde, K. E. (1964), *J. Biol. Chem. 239*, 2516.
Squire, P. G., and Li, C. H. (1961), *J. Amer. Chem. Soc. 83*, 3521.
Stafford, W. F., III, and Yphantis, D. A. (1972), *Biophys. J.* (in press).
Steiner, R. F. (1952), *Arch. Biochem. Biophys. 39*, 333.
Steiner, R. F. (1953a), *Arch. Biochem. Biophys. 44*, 120.
Steiner, R. F. (1953b), *Arch. Biochem. Biophys. 47*, 56.
Teller, D. C., Horbett, T. A., Richards, E. G., and Schachman, H. K. (1969), *Ann. N. Y. Acad. Sci. 146*, 66.
Van Holde, K. E., and Baldwin, R. L. (1958), *J. Phys. Chem. 62*, 734.
Yphantis, D. A. (1964), *Biochemistry 3*, 297.

Amino Acid Sequence of Monkey Amyloid Protein A†

Mark A. Hermodson,* Robert W. Kuhn, Kenneth A. Walsh, Hans Neurath, Nils Eriksen, and Earl P. Benditt

ABSTRACT: The amino acid sequence of amyloid protein A was determined. This protein was isolated from the liver of a monkey (*Macaca mulatta*) afflicted with amyloidosis. Amyloid protein A contains 76 amino acid residues in a single polypeptide chain devoid of disulfide bonds. Sequenator analysis of the whole protein and of a large fragment derived by cleavage with cyanogen bromide established the sequence of all but the six carboxyl-terminal residues. These were ordered by degradation with yeast protease C and by manual Edman degradation. The amino acid sequence of amyloid protein A bears no resemblance to the sequence of any protein of known function.

Amyloid substance is a complex proteinaceous material found in various tissues of patients and animals with the disease amyloidosis. Recent evidence indicates that there are two chemically distinct classes of amyloid substance: one (class A) occurs in individuals with any of several chronic inflammatory conditions while the other (class B) occurs in individuals with tumors or with no preexistent disease (Benditt and Eriksen, 1971).

A major protein constituent of the amyloid substance in inflammation-related amyloidosis has been designated "amyloid protein A." We have recently reported the amino-terminal sequence of this protein isolated from the livers of a human and a monkey afflicted with chronic inflammatory disease (Benditt *et al.*, 1971). Proteins from these two species show a high degree of sequence identity: they differ in only two positions in the 24 amino-terminal amino acid residues

† From the Departments of Biochemistry and Pathology, University of Washington School of Medicine, Seattle, Washington 98195. *Received April 13, 1972.* This work has been supported by research grants from the National Institutes of Health (GM-15731, HE-03174, and GM-13543) and the American Cancer Society (NP-18N).